Earth and Planetary Science Letters 333-334 (2012) 226–237

Contents lists available at SciVerse ScienceDirect

Earth and Planetary Science Letters

journal homepage: www.elsevier.com/locate/epsl

# Chemical heterogeneity in the upper mantle recorded by peridotites and chromitites from the Shetland Ophiolite Complex, Scotland

Brian O'Driscoll [a,*], James M.D. Day [b,c], Richard J. Walker [c], J. Stephen Daly [d], William F. McDonough [c], Philip M. Piccoli [c]

[a] School of Physical and Geographical Sciences, Keele University, Keele ST5 5BG, UK
[b] Geosciences Research Division, Scripps Institution of Oceanography, La Jolla, CA 92093-0244, USA
[c] Department of Geology, University of Maryland, College Park, MD 20742, USA
[d] UCD School of Geological Sciences, University College Dublin, Belfield, Dublin 4, Ireland

ARTICLE INFO

*Article history:*
Received 27 January 2012
Received in revised form
27 March 2012
Accepted 31 March 2012
Editor: B. Marty

*Keywords:*
mantle heterogeneity
melt depletion
Os isotopes
highly siderophile elements
Shetland Ophiolite Complex

ABSTRACT

The timing, causes and extent of mantle heterogeneity preserved in the ~492 Ma Shetland Ophiolite Complex (Scotland) are evaluated using Re–Os isotope and whole rock highly siderophile element (HSE: Os, Ir, Ru, Pt, Pd, Re) abundance measurements of a suite of eight chromitites and 21 serpentinised harzburgites and dunites. Shetland dunites have more variable initial $^{187}Os/^{188}Os$, as well as absolute and relative abundances of the HSE, compared to spatially associated harzburgites. As is common for ophiolitic peridotites, the harzburgites ($\gamma_{Os492Ma}$ of −5.3 to +2.6) preserve evidence for a Mesoproterozoic depletion event, but are dominated by contemporary chondritic, ambient upper mantle compositions. The dunites have $\gamma_{Os492Ma}$ values ranging between −3.3 and +12.4, reflecting dunite formation by higher degrees of melt interaction with mantle rock than for the spatially associated harzburgites.

Chromitite seams from three locations separated by < 500 m have a large range in HSE concentrations (e.g., 0.09 to ~2.9 μg $g^{-1}$ Os) with initial $\gamma_{Os492Ma}$ values ranging only from +0.48 to +3.95. Sulphides, arsenides and platinum-group minerals are the primary hosts for the HSE in the chromitites. Their isotopic variations reflect initial isotopic heterogeneity in their primary magmatic isotopic signatures. Coupled with field observations that support chromitite formation in concentrated zones of enhanced melt flow, the isotopic dichotomy between the harzburgites and the chromitites suggests that chromitite $^{187}Os/^{188}Os$ compositions may better approximate the upper limit, rather than an average value, of the bulk convecting upper mantle.

The Shetland peridotite compositions reflect protracted melt depletion (low-$Al_2O_3$) and melt percolation events in a supra-subduction zone (SSZ) setting at ~492 Ma, following an earlier (Mesoproterozoic) melt-depletion event. These results provide further evidence that ancient chemical complexities can be preserved in the upper mantle during ocean plate formation. Chromitites and peridotites from the Shetland Ophiolite Complex also attest to lithological and geochemical heterogeneities generated at scales of less than tens of metres during the formation of ancient oceanic lithosphere by high-degree SSZ melt extraction, percolation and during chromitite formation in the oceanic lithosphere.



## Introduction

Documentation of compositional variations in the upper mantle is crucial for understanding the geochemical evolution of the mantle (e.g., Workman and Hart, 2005). Oceanic abyssal peridotites reveal that the depleted upper mantle (DMM), the source of mid-ocean ridge basalts (MORB), is both chemically and isotopically heterogeneous, resulting from processes that include variable melt depletion, refertilisation and melt-rock reaction (e.g., Dick et al., 1984; Liu et al., 2009; Sharma and Wasserburg, 1996). The compositional variations preserved in abyssal peridotites and MORB indicate that mantle heterogeneity occurs at scales that range from the size of ocean basins to small (sub-cm) domains within the mantle, yet the timing of the creation of these heterogeneities continues to be vigorously debated (e.g., Alard et al., 2005; Dupré and Allègre, 1983; Luguet et al., 2007; Marchesi et al., 2010; Reisberg and Zindler, 1986; Standish et al., 2002).

Despite complex structural and petrological histories, the mantle sections of obducted ophiolite complexes can provide important evidence for mantle processes (e.g., Büchl et al., 2002;

* Corresponding author. Tel.: +44 1782 733184; fax: +44 1782 715261.
*E-mail address:* b.o'driscoll@esci.keele.ac.uk (B. O'Driscoll).

0012-821X/$ - see front matter © 2012 Elsevier B.V. All rights reserved.
http://dx.doi.org/10.1016/j.epsl.2012.03.035

Elthon, 1991; Kelemen et al., 1992; Pearce, 2003; Schulte et al., 2009; Shi et al., 2007; Snow et al., 1994; Snow and Reisberg, 1995). Compared to abyssal peridotites and MORB, ophiolites are particularly valuable for assessing the timing, causes and extent of mantle processes, as they allow field-based observation to be coupled with geochemical investigation of this otherwise inaccessible domain. Furthermore, ophiolites preserve a range of oceanic mantle (e.g., lherzolite, harzburgite, dunite) and crustal (e.g., gabbros, wehrlites, pyroxenites, basalts) lithologies; these attributes allow detailed assessment of the distribution and relative timing of mantle events and the processes that they preserve (e.g., Büchl et al., 2004a; Elthon, 1991; Hanghøj et al., 2010; Schulte et al., 2009; Tsuru et al., 2000; Walker et al., 2002).

A distinctive feature of ophiolites, which contrasts with abyssal peridotites, is the presence of chromitites ($\geq$60 modal % Cr-spinel), which typically form irregularly shaped podiform masses and occur in the region of the petrological Moho (e.g., Lago et al., 1982). These chromitite horizons are often associated with platinum-group element mineralisation (Marchesi et al., 2010; Melcher et al., 1997; Prichard et al., 1996). The timing and genesis of ophiolite podiform chromitites is controversial (e.g., Ballhaus, 1998; Melcher et al., 1997), but may be related to focused channelling of partial melts in a supra-subduction zone (SSZ) setting (Büchl et al., 2004b). Understanding the origin of podiform chromitites and contrasting their geochemical compositions with associated peridotites is important because it has been suggested that ophiolite chromitites may be more useful for constraining the Os isotopic evolution of the DMM (Walker et al., 2002), compared to MORB, abyssal peridotites, or even peridotites from ophiolites (e.g., Brandon et al., 2000; Gannoun et al., 2007; Hanghøj et al., 2010; Harvey et al., 2006; Liu et al., 2009; Luck and Allègre, 1991; Luguet et al., 2007; Marchesi et al.,

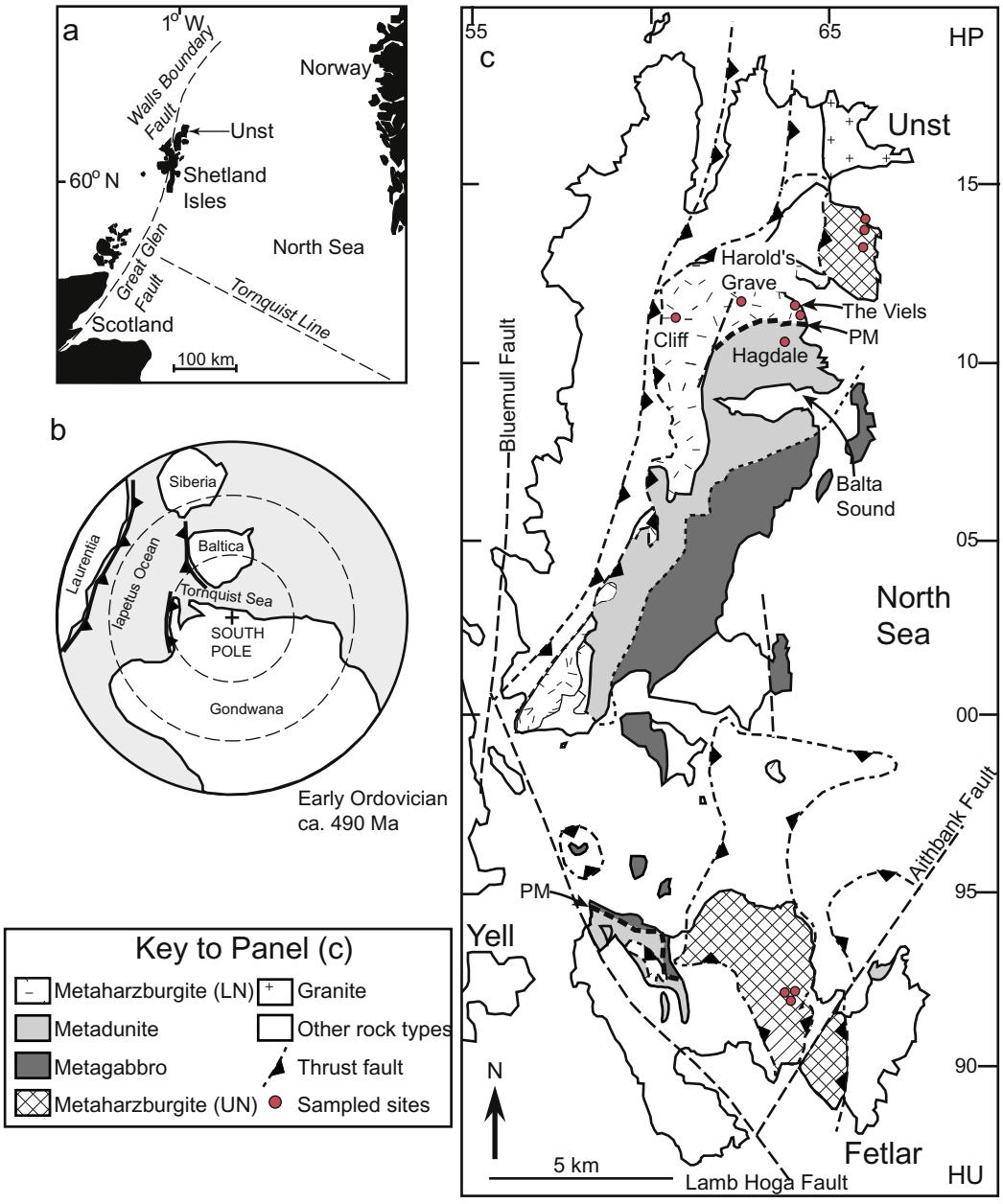


**Fig. 1.** (a) Regional map of the northern North Sea, showing the geographic location of the Shetland Ophiolite Complex. (b) Plate reconstruction illustrating the locations of the Laurentian foreland and Iapetus Ocean at ca. 490 Ma (modified from Woodcock and Strachan (2000)). (c) Simplified geological map of the Isles of Unst and Fetlar, illustrating positions of major lithological units of the ophiolite and the sample localities (adapted from Flinn, 2001). The trace of the petrological Moho (PM) is also highlighted as are the harzburgites of the upper (UN) and lower (LN) nappes. Grid lines are those of the UK National Grid (HP).

2010; Roy-Barman and Allègre, 1994; Schiano et al., 1997; Snow and Reisberg, 1995).

Here we report major-element and highly siderophile-element (HSE: Os, Ir, Ru, Pt, Pd, Re) abundances and $^{187}Re$–$^{187}Os$ data for a suite of peridotites and associated chromitites from the ~492 Ma Shetland Ophiolite Complex, Scotland (SOC; Spray and Dunning, 1991), in conjunction with detailed mineral-scale and outcrop observations. We investigate the causes of spatial and temporal geochemical variations within this portion of oceanic mantle and the effects of melt-depletion, melt-rock reaction and/or refertilisation. The HSE are particularly sensitive tracers of melt-depletion and melt-rock reactions because of the contrasting compatibilities of Os, Ir, Ru and Rh (I-PGE) relative to typically incompatible Pt, Pd, Re (P-PGE) and Au (P-PGE), and because of the utility of the Re–Os isotope system ($^{187}Re \rightarrow {}^{187}Os + \beta^-$; $\lambda = 1.67 \times 10^{-11}\ yr^{-1}$) to record the long-term, time-integrated behaviour of these elements (e.g., Allègre and Luck, 1980; Rudnick and Walker, 2009; Walker et al., 1989; Walker, 2009). We also assess the utility of podiform chromitite, compared with whole-rock silicates, for tracking the Os isotope evolution of the DMM, and use the new isotopic and elemental data to provide insights into the generation of podiform chromitites, including their tendency to concentrate the HSE.

## Geological background and samples

The SOC occurs as a stacked pair of variably serpentinised 'cold' ($<400^{\circ}C$) obduction nappes on the islands of Unst and Fetlar in the Shetland Islands, Scotland (Fig. 1a; Flinn and Oglethorpe, 2005). A zircon U-Pb crystallisation age from a plagiogranite vein cutting the upper portion of the SOC provides a minimum age of $492 \pm 3$ Ma (Spray and Dunning, 1991), with obduction along the sole thrust no later than $465 \pm 6$ Ma (Flinn et al., 1991; Spray, 1988). Westward emplacement of the ophiolite is thought to be related to arc collision and closure of the Iapetus Ocean, associated with the Grampian orogeny at ~470 Ma (Fig. 1b; Chew et al., 2010).

The SOC is an ideal location for studying the chemical and isotopic heterogeneity of the Iapetan upper mantle, as it preserves an extensive, undeformed section of mantle dunites, harzburgites and pyroxenites, as well as numerous podiform chromitites (Flinn and Oglethorpe, 2005). The ophiolite complex is tilted almost vertically, revealing a lowermost layer of harzburgite overlain by a 1–3 km thick dunite layer, and an uppermost olivine-deficient gabbro sequence (Fig. 1c). Dunites and harzburgites are intensely serpentinised and primary olivine ± orthopyroxene assemblages are seldom preserved. Irregular and laterally discontinuous podiform chromitite seams, up to 2 m thick, occur in the peridotites (Fig. 2a), and are most common immediately above and below the east-west trending petrological Moho on Unst (Fig. 1b) (Prichard and Lord, 1993). In these regions, the harzburgite contains numerous lenses and layers of dunite (cm to m scale) that strike subparallel to, or discordantly with, the petrological Moho (Fig. 2b).

Chromitite seams from three localities were examined. These seams run from west (Cliff) to east (Harold's Grave and Hagdale) in close proximity to the petrological Moho. Serpentinised harzburgites and dunites from both the lower and upper nappes on Unst and from the upper nappe on Fetlar were also investigated (Fig. 1c). Further sample location details can be found in Table S1. Cliff and Harold's Grave chromitites are known to contain high Pt and Pd concentrations (~60 $\mu g\ g^{-1}$ Pt+Pd; Prichard and Lord, 1993). Chromitite seams, 0.01–2 m thick, are laterally discontinuous on the scale of tens of metres. Seams are oriented broadly parallel to the petrological Moho, but at the outcrop scale are often complexly deformed, forming stock-work veins and patches that are highly discordant to the overall east-west structural trend. Chromitite seams are almost ubiquitously contained within dunite, rather than harzburgite, and accessory Cr-spinel is always present in greater amounts (up to 5 vol%) in dunite compared to harzburgite

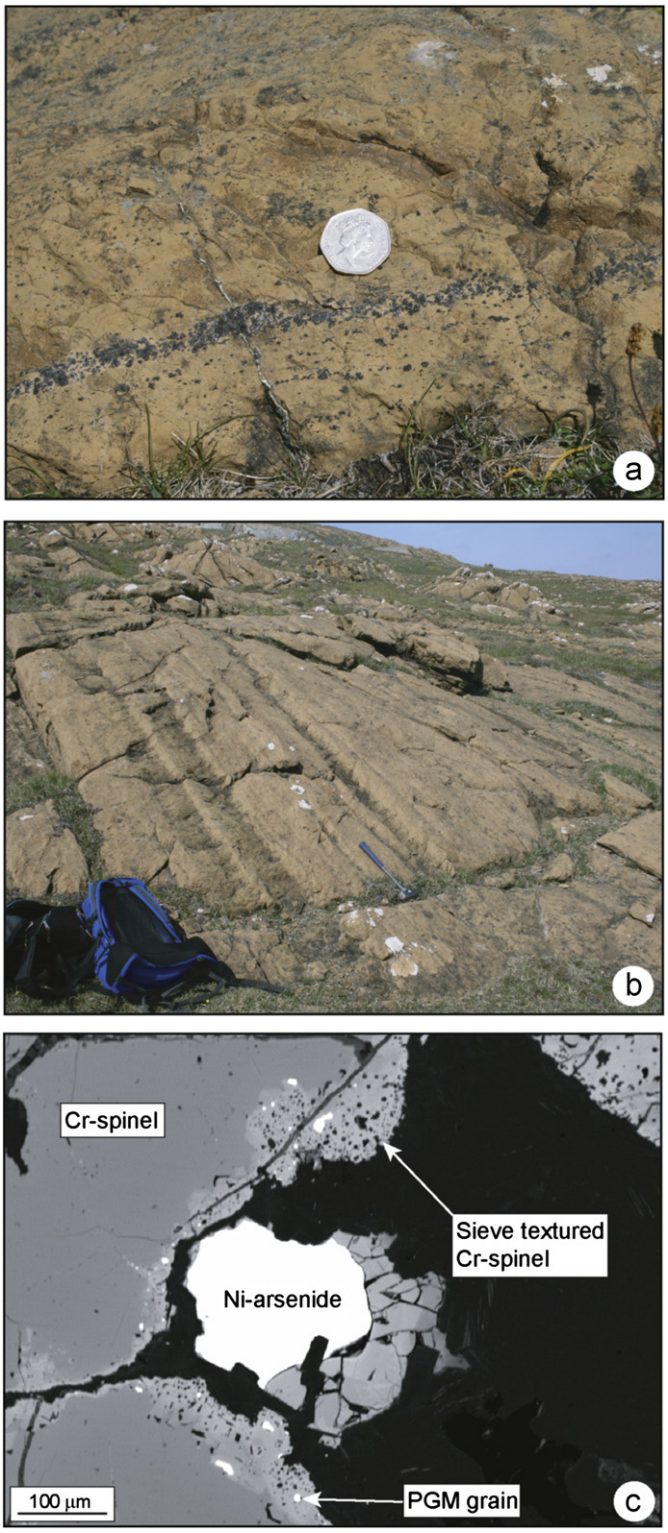


**Fig. 2.** (a) Field photograph of thin podiform chromitite seam (~2.5 cm diameter coin for scale). (b) Layering of harzburgite and dunite at the Viels locality, ~200 m below the petrological Moho. (c) Back scattered electron micrograph image of Cr-spinel crystals (light grey) with typical sieve-textured coronas adjacent to Ni-arsenide grain from the Cliff locality. Platinum-group minerals (highlighted), mostly sperrylite, are disseminated throughout these coronas.

**Table 1**
Re–Os isotope systematics and highly siderophile element abundance data for the Shetland Ophiolite Complex.

| Sample | Lithology | MgO (wt%) | $Al_2O_3$ (wt%) | Os (ng $g^{-1}$) | Ir (ng $g^{-1}$) | Ru (ng $g^{-1}$) | Pt (ng $g^{-1}$) | Pd (ng $g^{-1}$) | Re (ng $g^{-1}$) | Os/Ir | Pt/Ir | Pd/Ir | $^{187}Re/^{188}Os$ | $\pm 2\sigma$ | $^{187}Os/^{188}Os$ | $\pm 2\sigma$ | $\gamma_{Os(492\ Ma)}$ |
|---|---|---|---|---|---|---|---|---|---|---|---|---|---|---|---|---|---|
| C1 | Chromitite | 22.8 | 6.14 | 1997 | 7679 | – | – | – | 0.4682 | 0.260 | – | – | 0.00113 | 0.00003 | 0.129210 | 0.000028 | 3.94 |
| *Replicate* | | | | 1940 | 10760 | 16680 | 79420 | 110300 | 0.3477 | 0.180 | 7.38 | 10.3 | 0.00086 | 0.00003 | 0.129217 | 0.000005 | 3.95 |
| C2 | Chromitite | 25.8 | 8.34 | 1402 | 3289 | 5908 | – | – | 1.090 | 0.426 | – | – | 0.00375 | 0.00011 | 0.129227 | 0.000008 | 3.94 |
| *Replicate* | | | | 1329 | 5727 | 7935 | 44550 | 48470 | 0.5328 | 0.232 | 7.78 | 8.46 | 0.00193 | 0.00006 | 0.129229 | 0.000004 | 3.95 |
| C3 | Chromitite | 23.2 | 8.00 | 2935 | 8821 | 20060 | – | – | 7.918 | 0.333 | – | – | 0.01300 | 0.00039 | 0.129250 | 0.000006 | 3.90 |
| *Replicate* | | | | 2810 | 11680 | 20270 | 96620 | 156000 | 0.4160 | 0.241 | 8.27 | 13.4 | 0.00071 | 0.00002 | 0.129208 | 0.000005 | 3.94 |
| C4 | Dunite | 49.9 | 0.08 | 4.581 | 3.007 | 5.68 | 1.369 | 0.672 | 0.013 | 1.52 | 0.455 | 0.223 | 0.014 | 0.003 | 0.13834 | 0.00020 | 11.2 |
| *Replicate* | | | | 5.694 | 2.463 | 7.71 | 4.622 | 1.219 | 0.0089 | 2.31 | 1.88 | 0.495 | 0.0075 | 0.002 | 0.13975 | 0.00020 | 12.4 |
| C5 | Harzburgite | 45.4 | 0.59 | 4.468 | 3.588 | 8.70 | 8.091 | 4.613 | 0.025 | 1.25 | 2.25 | 1.29 | 0.027 | 0.005 | 0.12479 | 0.00020 | 0.2 |
| *Replicate* | | | | 3.859 | 2.558 | 6.73 | 4.670 | 2.598 | 0.010 | 1.51 | 1.83 | 1.02 | 0.013 | 0.003 | 0.12458 | 0.00020 | 0.1 |
| HG1 | Chromitite | 14.9 | 16.2 | 701.5 | 546.1 | 2356 | 459.2 | 111.9 | 0.0161 | 1.28 | 0.841 | 0.205 | 0.000111 | 0.000003 | 0.125542 | 0.000042 | 1.00 |
| HG2 | Chromitite | 17.5 | 14.3 | 1693 | 1485 | 3440 | 1220 | 120.9 | 0.1223 | 1.14 | 0.822 | 0.081 | 0.00035 | 0.00001 | 0.124896 | 0.000001 | 0.48 |
| *Replicate* | | | | 996.6 | 666.8 | 3000 | 846.2 | 65.12 | 0.1168 | 1.49 | 1.27 | 0.098 | 0.00056 | 0.00002 | 0.125298 | 0.000001 | 0.80 |
| HG3 | Chromitite | 16.0 | 13.7 | 1117 | 1012 | 2999 | 1124 | 122.1 | 0.0473 | 1.10 | 1.11 | 0.121 | 0.000204 | 0.000006 | 0.125229 | 0.000006 | 0.75 |
| HF1 | Chromitite | 20.4 | 16.1 | 86.91 | 71.25 | 160.1 | 15.7 | 23.1 | 0.0636 | 1.22 | 0.220 | 0.325 | 0.00353 | 0.00011 | 0.125996 | 0.000005 | 1.34 |
| HF2 | Chromitite | 20.3 | 16.4 | 90.42 | 64.72 | 144.7 | 6.0 | 26.7 | 0.0897 | 1.40 | 0.093 | 0.413 | 0.00478 | 0.00014 | 0.126046 | 0.000023 | 1.37 |
| HF3 | Dunite | 48.9 | 0.46 | 0.398 | 0.407 | 1.759 | 0.030 | 2.982 | 0.0497 | 0.978 | 0.074 | 7.32 | 0.602 | 0.018 | 0.12950 | 0.00013 | 0.2 |
| V1 | Dunite | 48.2 | 0.30 | 5.886 | 3.885 | 12.04 | 4.571 | 4.170 | 0.0842 | 1.51 | 1.18 | 1.07 | 0.069 | 0.002 | 0.12649 | 0.00007 | 1.3 |
| V2 | Min. Dunite | 45.6 | 1.22 | 41.68 | 38.40 | 56.11 | 407.4 | 644.9 | 14.84 | 1.09 | 10.6 | 16.8 | 1.719 | 0.052 | 0.14178 | 0.00002 | 2.7 |
| V3 | Harzburgite | 45.3 | 0.36 | 3.657 | 3.849 | 6.018 | 5.764 | 9.870 | 0.0871 | 0.950 | 1.50 | 2.56 | 0.115 | 0.003 | 0.12306 | 0.00009 | −1.8 |
| *Replicate* | | | | 3.713 | 4.352 | 7.101 | 5.520 | 9.870 | 0.0606 | 0.853 | 1.27 | 2.27 | 0.079 | 0.002 | 0.12518 | 0.00010 | 0.2 |
| V4 | Dunite | 47.0 | 0.13 | 5.053 | 4.959 | 8.094 | 5.079 | 9.149 | 0.0697 | 1.02 | 1.02 | 1.84 | 0.066 | 0.002 | 0.12079 | 0.00006 | −3.3 |
| V6 | Harzburgite | 45.7 | 0.28 | 2.614 | 2.626 | 3.846 | 3.499 | 3.182 | 0.0335 | 1.00 | 1.33 | 1.21 | 0.062 | 0.002 | 0.11821 | 0.00008 | −5.3 |
| AV1 | Harzburgite | 45.2 | 0.35 | 3.931 | 2.259 | 5.629 | 5.884 | 1.946 | 0.0457 | 1.74 | 2.60 | 0.861 | 0.056 | 0.002 | 0.12649 | 0.00010 | 1.4 |
| AV4D | Dunite | 47.7 | 0.37 | 3.451 | 3.270 | 5.381 | 18.69 | 37.17 | 1.992 | 1.06 | 5.72 | 11.4 | 2.789 | 0.084 | 0.15018 | 0.00002 | 2.4 |
| AV4H | Harzburgite | 46.8 | 0.28 | 3.715 | 2.919 | 7.248 | 5.621 | 7.612 | 0.2807 | 1.27 | 1.93 | 2.61 | 0.364 | 0.011 | 0.12393 | 0.00010 | −2.7 |
| AV5* | Dunite | 49.2 | 0.38 | 2.854 | 0.743 | 2.982 | 2.146 | 1.123 | 0.3179 | 3.84 | 2.89 | 1.51 | 0.537 | 0.010 | 0.12985 | 0.00010 | 0.9 |
| UN 1* | Harzburgite | 45.1 | 0.56 | 1.911 | 1.198 | 1.983 | 1.968 | 0.721 | 0.0459 | 1.60 | 1.64 | 0.602 | 0.116 | 0.002 | 0.12847 | 0.00010 | 2.6 |
| UN 2* | Harzburgite | 46.0 | 0.95 | 2.632 | 0.642 | 1.055 | 3.071 | 0.787 | 0.0226 | 4.10 | 4.78 | 1.23 | 0.041 | 0.008 | 0.12527 | 0.00010 | 0.5 |
| UN 3 | Harzburgite | 45.9 | 0.70 | 5.462 | 3.075 | 6.109 | 4.737 | 1.269 | 0.0162 | 1.78 | 1.54 | 0.413 | 0.014 | 0.003 | 0.12044 | 0.00020 | −3.2 |
| *Replicate* | Harzburgite | | | 2.359 | 3.121 | 7.464 | 12.00 | 1.914 | 0.0147 | 0.756 | 3.84 | 0.613 | 0.030 | 0.006 | 0.12060 | 0.00020 | −3.2 |
| UN 4a | Harzburgite | 44.4 | 0.66 | 4.204 | 4.177 | 7.509 | 12.48 | 5.140 | 0.0181 | 1.01 | 2.99 | 1.23 | 0.021 | 0.004 | 0.12697 | 0.00020 | 2.0 |
| *Replicate* | Harzburgite | | | 8.423 | 4.027 | 8.608 | 14.58 | 6.130 | 0.0663 | 2.09 | 3.62 | 1.52 | 0.038 | 0.008 | 0.12748 | 0.00020 | 2.3 |
| Fet 3 | Dunite | 47.9 | 0.87 | 0.503 | 0.222 | 1.247 | 0.278 | 0.199 | 0.880 | 2.26 | 1.25 | 0.894 | 8.47 | 0.17 | 0.16667 | 0.00013 | −22.0 |
| Fet 4 | Dunite | 49.1 | 0.09 | 0.570 | 0.626 | 0.656 | 1.086 | 1.410 | 0.373 | 0.910 | 1.73 | 2.25 | 3.16 | 0.063 | 0.13494 | 0.00013 | −12.4 |
| Fet 6* | Harzburgite | 43.1 | 1.56 | 3.621 | 2.933 | 3.262 | 9.123 | 9.920 | 0.170 | 1.23 | 3.11 | 3.38 | 0.226 | 0.005 | 0.12520 | 0.00010 | −0.8 |
| Fet 7 | Dunite | 49.4 | 0.06 | 3.247 | 1.436 | 12.38 | 8.071 | 25.14 | 0.143 | 2.26 | 5.62 | 17.5 | 0.212 | 0.004 | 0.13533 | 0.00010 | 7.5 |
| Fet 8* | Harzburgite | 43.9 | 0.89 | 4.397 | 2.506 | 4.036 | 6.252 | 5.369 | 0.139 | 1.75 | 2.49 | 2.14 | 0.153 | 0.003 | 0.12509 | 0.00010 | −0.4 |
| GP13 | SRM Peridotite | | | 3.882 | 3.332 | 7.173 | 5.652 | 5.243 | 0.2890 | 1.17 | 1.70 | 1.57 | 0.359 | 0.011 | 0.12595 | 0.00001 | |

Cells marked by '–' signify measurements that were not carried out.

(typically $<1$ vol%). The Cliff locality is directly adjacent ($\sim$100 m) to the purported basal thrust of the ophiolite, a relationship previously used to account for the anomalously high HSE and As contents at this locality (Prichard and Lord, 1993).

## Methods

Rhenium–osmium isotope and HSE (Os, Ir, Ru, Pt, Pd, Re) abundance measurements were performed at the University of Maryland, College Park, using protocols outlined previously (e.g., Day et al., 2010; O'Driscoll et al., 2009). Briefly, 0.1–1 g of whole-rock powder was digested in a 1:2 mix of 12 mol $L^{-1}$ HCl and 16 mol $L^{-1}$ $HNO_3$ at $>260$ °C for $>72$ h, with isotopically enriched ($^{99}Ru$, $^{105}Pd$, $^{185}Re$, $^{190}Os$, $^{191}Ir$, $^{194}Pt$) spikes. Osmium was purified by solvent extraction and micro-distillation. Measurement of Os was performed in negative ion mode using either a *VG Sector 54* or *ThermoFisher Triton* thermal ionisation mass spectrometer employing static measurement with faraday detectors for chromitites, or peak-jumping with a single secondary electron multiplier (SEM) on the Triton for all other samples. External precision for $^{187}Os/^{188}Os$ by static measurement of 35 ng loads of the UMCP Johnson and Matthey (J–M) standard was 0.13‰ ($0.113820 \pm 13$; $n=6$; $2\sigma$) using the *Sector 54*, and 0.06‰ ($0.113788 \pm 7$; $n=3$; $2\sigma$) for the Triton. Measurements of 0.35–3.5 ng loads of the UMCP J–M standard using the SEM on the Triton gave external precision of 1.9‰ ($0.11380 \pm 20$; $n=10$ $2\sigma$); all reported Os isotope ratios are normalised to $^{187}Os/^{188}Os=0.11380$ for the UMCP J–M standard. Rhenium, Pd, Pt, Ru and Ir were purified using anion exchange separation techniques and were measured using a *ThermoFisher Element 2* ICP-MS. External reproducibility ($2\sigma$) was better than 0.5% for Re, Ir, Pt, Pd, and Ru. Average total procedural blanks ($n=4$) gave $^{187}Os/^{188}Os=0.128 \pm 0.009$, and (in pg) $0.7 \pm 0.9$ Re, $12 \pm 15$ Pd, $5.8 \pm 2.7$ Pt, $2.0 \pm 1.5$ Ru, $4.9 \pm 1.9$ Ir, and $0.14 \pm 0.05$ Os. Blank corrections were applied and are $<1\%$ for Os, Ir, Ru, Pt and Pd. Blank corrections for Re represent $<1\%$ (e.g., V2; Cr-spinel-rich dunite) to 30% (e.g., HG-1; chromitite).

Accuracy and reproducibility was monitored by analysis of the GP13 peridotite standard. These analyses show good agreement with previous data from our laboratory (Puchtel et al., 2008) and with results published from other laboratories (Day et al., 2008) (Table 1). Replicate analyses resulted in $^{187}Os/^{188}Os$ reproducibility of 0.3% or better for chromitites and $\sim$2% for the V3 harzburgite. Reproducibility of HSE concentration analyses are better than 10% in most cases, but are apparently affected by 'nuggeting' of HSE-rich trace phases for some powders (e.g., Becker et al., 2006).

In situ laser-ablation ICP-MS analysis of sulphides and arsenides were performed at the University of Maryland using a *New Wave* 213 nm laser-ablation system coupled to the *Element 2* ICP-MS, as described in O'Driscoll et al. (2009). Electron microprobe analyses of Cr-spinel, arsenide and sulphide were performed at the University of Maryland using a *JEOL JXA 9800* electron probe micro-analyser, and whole-rock major and trace element analyses were performed at the University of Leicester, UK using a *PANalytical Axios Advanced XRF* spectrometer. Further details of these methods are presented in the *Supplementary Materials*.

## Results

### *Cr-spinel, sulphide and arsenide mineral compositions*

Chromium-spinel grains in SOC chromitite seams are predominantly relatively fresh, though altered 'sieve' textured rims and fractures are common, especially at Cliff. Unaltered Cr-spinels have compositions ranging between picrochromite ($MgCr_2O_4$) and chromite ($FeCr_2O_4$), with Mg-rich chromites reflecting primary compositions (cf. Droop, 1987). Mg# ($Mg/[Mg+Fe^{2+}] \times 100$) and Cr# ($Cr/[Cr+Al]$) molar values in the Cr-spinels are 24–79.5 and 0.55–0.98, respectively (*Table S2, Fig. S1*). The sieve-textured coronas surrounding Cr-spinel crystals at all three chromitite localities (Fig. 2c) correspond to $Al^{3+}$ depleted and correspondingly $Fe^{3+}$ and $Cr^{3+}$ enriched compositions.

Minor amounts of sulphide (Harold's Grave and Hagdale Quarry) or arsenide (Cliff) typically occur in close textural association with Cr-spinel crystals in the chromitites, and are usually separated from fresh Cr-spinel by sieve textured coronas that contain HSE-bearing phases (Fig. 2c; e.g., Prichard and Tarkian, 1988). Layers and lenses of sulphide-enriched dunites are common close to the petrological Moho, and particularly adjacent to chromitite seams. Pentlandite ($[Fe,Ni]_9S_8$; in quantities up to 5 vol%, but typically $\leq 0.5$ vol%) is the dominant sulphide, accompanied by minor heazlewoodite ($Ni_3S_2$) or millerite (NiS). The Cliff chromitites occur in a pod-like body of dunite (Prichard and Lord, 1993), and are the only rocks observed in the ophiolite that contain abundant Ni-arsenide ($\leq 5$ vol%), with little or no corresponding sulphide. Harzburgites are typically barren of sulphide or visible HSE-rich alloy grains.

HSE and minor element abundances for Cr-spinels, sulphides and arsenides are presented in Table S3 and Figures S2 and S3. HSE abundances for chromite grains in all four localities are generally below limits of detection. Sieve-textured rims on Cr-spinel are relatively enriched in Ni, Co, Zn and Pb as compared with fresh Cr-spinel. Pentlandite accounts for much of the HSE budget in the V2 dunite. Arsenide phases dominate the Os, Ir, Ru, Pt and Pd budget of the Cliff chromitites, with concentrations of up to 34 μg $g^{-1}$ Os, 89 μg $g^{-1}$ Ir and 655 μg $g^{-1}$ Pd. Ni-arsenide or sulphide minerals alone cannot account for the high Ir and Pt concentrations of these samples; based on LA-ICP-MS rasters, these elements are probably retained in the groundmass serpentinite as sub-micron HSE-rich trace phases (Fig. S3).

### *Whole-rock major- and minor-element abundances*

Peridotites all have high loss-on-ignition (LOI; *Table S1*), with dunites (mean $13.5 \pm 2.4$; $n=10$; $2\sigma$; range 11.7–15.9 wt%) having slightly higher LOI than harzburgites (mean $11.6 \pm 2.4$; $n=11$; $2\sigma$; range 8.8–13.3 wt%), similar to peridotites from other ophiolite complexes (e.g., Büchl et al., 2004a; Hanghøj et al., 2010; Schulte et al., 2009). Anhydrous peridotite compositions have high Mg-numbers (0.88–0.90) and Ni contents (1800–4950 μg $g^{-1}$), and low $Al_2O_3$ (0.06–1.56 wt%). Broad negative correlations occur between MgO and $Al_2O_3$, similar to whole-rock compositions reported from other ophiolites (*Fig. S4; Table S1*). Variable Cr contents (1390–20,100 μg $g^{-1}$) reflect Cr-spinel preserved in harzburgites and dunites, with the dunites having generally higher Cr and Ni contents than harzburgites.

### *Whole-rock HSE abundances and $^{187}Os/^{188}Os$*

#### *Chromitites*

HSE concentrations are lowest in Hagdale chromitites, which have pronounced depletions in Pt relative to Ru and Pd on a chondrite-normalised plot, similar to the 'global compilation' of ophiolite chromitites (Büchl et al., 2004b). Harold's Grave chromitites are also characterised by negatively sloping HSE patterns, whereas Cliff chromitites have the highest HSE abundances, with positively sloping patterns of Os, Ir, Ru, Pt, and Pd (Fig. 3a). Cliff chromitites contain HSE abundances of 11.7 μg $g^{-1}$ Ir, 20.3 μg $g^{-1}$ Ru, 96.6 μg $g^{-1}$ Pt, and 156 μg $g^{-1}$ Pd. Chromitites from each locality are characterised by a restricted range of measured

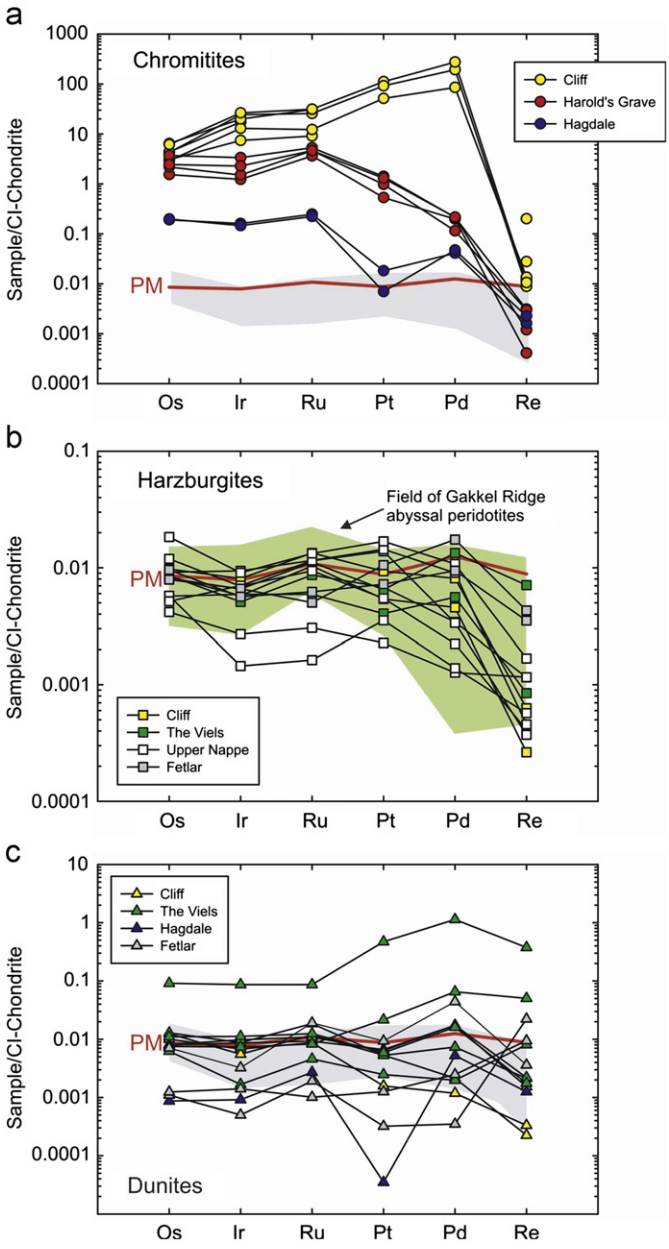


**Fig. 3.** Chondrite-normalised (CI-type Orgueil; Horan et al., 2003) highly siderophile element (HSE) patterns for (a) chromitites (from the Harold's Grave, Hagdale, and Cliff localities) (b) harzburgites and (c) dunites, in the Shetland Ophiolite Complex. The grey band in (a) and (c) illustrates the range of SOC harzburgite data for comparison with chromitites and dunites. The primitive mantle (PM) estimate in each panel is from Becker et al. (2006). The range of Gakkel Ridge abyssal peridotite HSE compositions are included in (b) for comparison (data from Liu et al., 2009, and references therein).

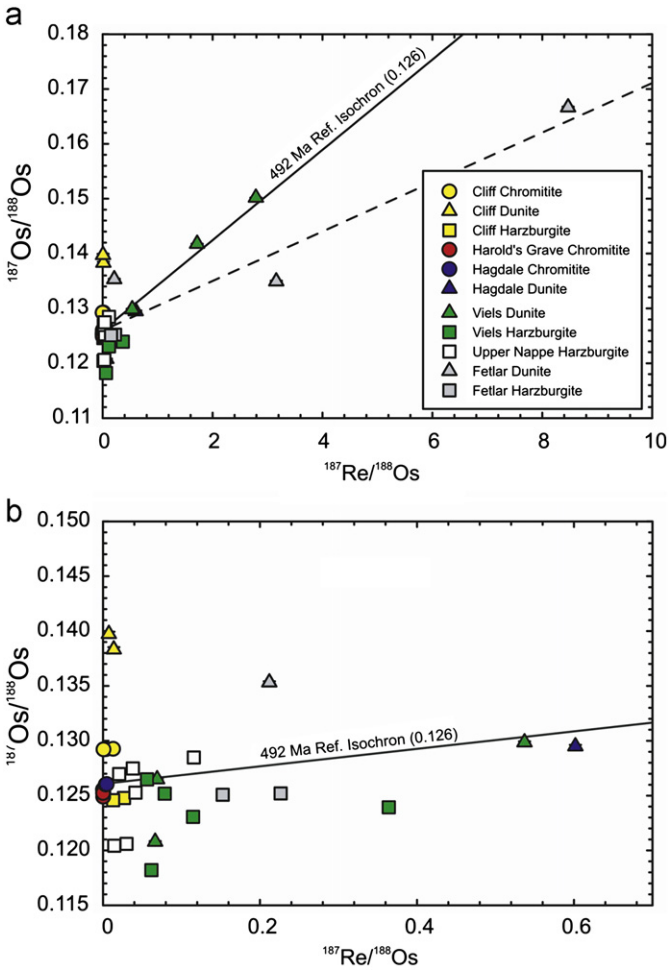


**Fig. 4.** (a) $\gamma_{Os492Ma}$ versus Os concentration for all samples. (b) $^{187}Re/^{188}Os$ versus $^{187}Os/^{188}Os$ for peridotites and chromitites from the Shetland Ophiolite Complex. Also shown is the 492 Ma reference isochron tied to $^{187}Os/^{188}Os = 0.126$. The two dunites from Fetlar with low calculated initial ratios fall along a best fit errorchron defined by the five Fetlar peridotites with an age of $270 \pm 160$ Ma and initial $^{187}Os/^{188}Os$ of $0.126 \pm 0.01$ that may provide a hint as to when open-system behaviour occurred for these samples (dashed line). (b) Expanded view of low $^{187}Re/^{188}Os$ chromitite and peridotite samples.

$^{187}Os/^{188}Os$ (Harold's Grave $= 0.12524 \pm 53$: $n=4$; Hagdale $= 0.12602 \pm 7$: $n=2$; Cliff $= 0.12922 \pm 3$: $n=6$; $2\sigma$) and low $^{187}Re/^{188}Os$ (0.0001–0.013) (Fig. 4a). Consequently, $\gamma_{Os492Ma}$ values (Table 1) for the chromitite seams (Cliff: $+3.90 \pm 0.01$ to $+3.94 \pm 0.04$; Harold's Grave: $+0.48 \pm 0.002$ to $+1.00 \pm 0.068$; Hagdale: $+1.34 \pm 0.008$ to $+1.37 \pm 0.036$) are precise and not subject to meaningful uncertainty resulting from age corrections.

*Peridotites*

Harzburgites have Os, Ir, Ru, Pt, and Pd abundances (1.9–8.4 ng $g^{-1}$ Os, 2.0–14.6 ng $g^{-1}$ Pt), comparable to that of the primitive mantle (PM) composition (cf., Becker et al., 2006), whereas Re concentrations are mostly lower than PM (0.01–0.28 ng $g^{-1}$) (Fig. 3b). The harzburgites have a restricted range in measured $^{187}Os/^{188}Os$ (0.1182–0.1285), with low, sub-chondritic $^{187}Re/^{188}Os$ (0.01–0.36) and $\gamma_{Os492Ma}$ of $-5.3$ to $+2.6$. Dunites span a much wider range of HSE concentrations than the harzburgites, have more radiogenic $^{187}Os/^{188}Os$ (0.1208–0.1667), generally higher $^{187}Re/^{188}Os$ (0.01–8.47), and define a broad range of $\gamma_{Os492Ma}$ values ($-22$ to $+12.4$). The two dunites with low calculated $\gamma_{Os492Ma}$ values of $-22.0$ and $-12.4$ (Fet 3 and Fet 4) have $^{187}Re/^{188}Os$ values that are well above chondritic, and thus, are probably biased to anomalously low $\gamma_{Os492Ma}$ values as a result of later-stage Re addition. Consequently, these anomalous initial ratios are not significant with respect to mantle compositions at the time of formation. Excluding these samples, $\gamma_{Os492Ma}$ values for the dunites range from $-3.3$ to $+12.4$. Several of the Viels dunites lie along a 492 Ma reference isochron with an initial $^{187}Os/^{188}Os$ value of $\sim 0.126$; close to the estimated $^{187}Os/^{188}Os$ value for PM at that time (Fig. 4b).

## Discussion

### *Effect of serpentinisation on Shetland Ophiolite Complex peridotites*

Because the SOC is variably but pervasively serpentinised, a key issue to address is the effect that late-stage and low-temperature alteration had on primary magmatic HSE abundances and Os isotopic compositions. Previous studies report that serpentinisation tends to stabilise platinum-group alloy grains, the dominant hosts of the HSE (Büchl et al., 2002; Liu et al., 2009; Lorand et al., 1993; Snow and Schmidt, 1998; Walker et al., 2002). Conversely, seawater alteration has been associated with mobilisation of Re, although no correlation between Re content and degree of alteration has been found (cf., Harvey et al., 2006; Liu et al., 2009). Changes in the primary sulphides, important carriers of Re and some HSE, can convert pentlandite to 'reduced' sulphide varieties, such as heazlewoodite (Sato and Ogawa, 2000), potentially mobilising the HSE. Pentlandite is the dominant sulphide in the Shetland dunites, with trace amounts of heazlewoodite and millerite, suggesting that the latter phases do not control the HSE compositions. In the harzburgites, sulphides are rare to absent, and the chondrite-normalised HSE patterns are consistent with the range of HSE abundances observed in the modern-day, ultra-slow-spreading Gakkel Ridge abyssal peridotites, which preserve the global range of HSE abundances measured to date in abyssal peridotites (Fig. 3).

Given that abyssal peridotites typically show comparable serpentinisation and alteration (e.g., variable serpentinisation and similar LOI values) as observed in the SOC peridotites, it is possible that such processes may have acted to modify the HSE compositions of the SOC peridotites (cf., Liu et al., 2009; Luguet et al. 2003; Schulte et al. 2009). In plots of Ir concentration versus Os/Ir, Ru/Ir, Pt/Ir, Pd/Ir and Re/Ir, the majority of Shetland harzburgites and dunites fall within the range of inter-element ratios defined by a global compilation of data for abyssal peridotites (Fig. 5). In contrast, some of the Shetland dunites have high Os/Ir, Pt/Ir, Pd/Ir and Re/Ir at low Ir concentrations, consistent with pervasive infiltration of mobilised sulphide-rich fluids (see Section 5.2). These fluids may also have produced the high Re/Os measured in some dunites (e.g., V2). However, previous work on abyssal peridotites found that serpentinisation did not significantly alter HSE compositions (Harvey et al., 2006; Liu et al., 2009). Lack of evidence of HSE mobilisation during serpentinisation, combined with the similarity of abyssal peridotite HSE contents to Shetland harzburgites and continental lithospheric mantle peridotites (Becker et al. 2006), indicates there is limited justification for invoking serpentinisation as a process that strongly disturbed primary magmatic HSE compositions for most of the SOC peridotites. Indeed, the Shetland peridotites predominantly have low Re/Os (except Fet 3 and 4) and are interpreted as retaining their Re–Os isotope systematics imparted by primary magmatic processes at ~492 Ma (Fig. 4).

### *Supra-subduction zone processes and dunite formation in ophiolites*

The SOC formed during supra-subduction zone (SSZ) melting at ca. 492 Ma, associated with the subduction of the Iapetus Ocean (Flinn, 2001; Prichard et al., 1996; Spray and Dunning, 1991). Field relations in the mantle section of the ophiolite reveal the presence of complexly inter-layered harzburgites and dunites consistent with variable to high degrees of partial melting. The low $Al_2O_3$ contents of Shetland peridotites ($< 1.6$ wt% $Al_2O_3$, anhydrous corrected) and typically high Cr# in chromitite Cr-spinel (0.49–0.98) are consistent with their being melt residues, rather than cumulates. Dunite layers in the mantle sections of SSZ ophiolites are commonly considered to represent palaeo-melt channels, resulting from high degrees of melt-rock interaction

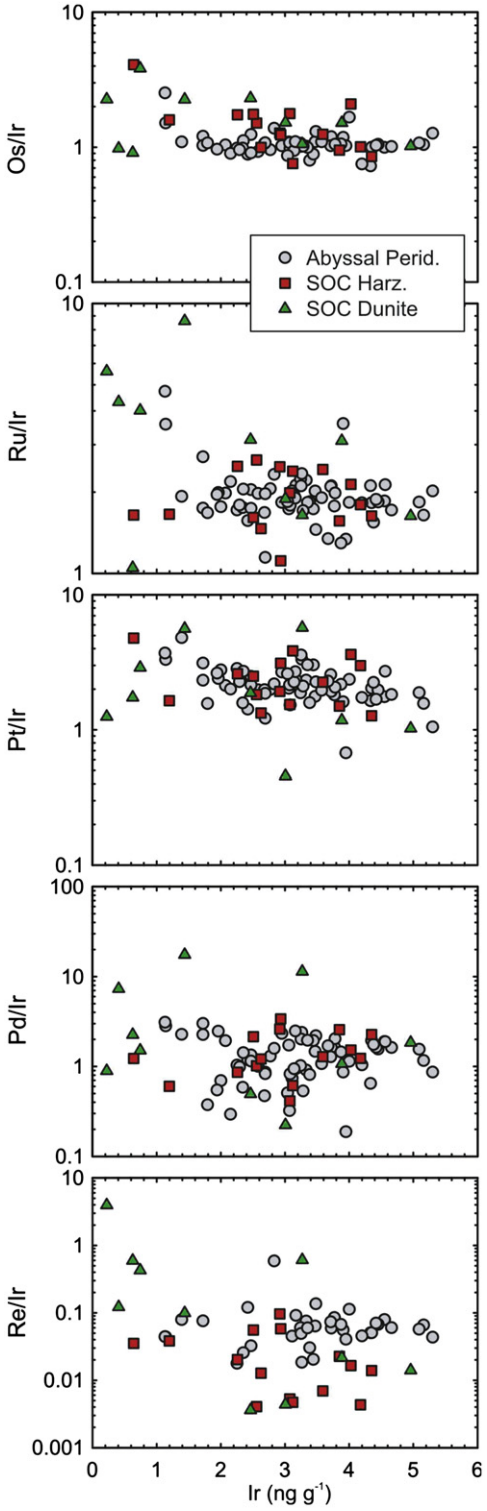


**Fig. 5.** Plots of ratios of the HSE, Os/Ir, Ru/Ir, Pt/Ir, Pd/Ir and Re/Ir against Ir concentration (ng $g^{-1}$). Also included in each panel for reference are abyssal peridotite compositions (data from Liu et al., 2009, and references therein).

associated with enhanced (fluid-assisted) melt generation (Büchl et al., 2004b; Kelemen et al., 1995; Quick, 1981). The presence of complex interlayering of dunite and harzburgite below the petrological Moho on the Isle of Unst, together with a thick (1–3 km; Flinn, 2001) layer of dunite above the petrological Moho provides compelling evidence for melt percolation and extraction in the SOC upper mantle during high flux melting in a SSZ setting.

Globally, dunite 'channel' formation has been taken by some workers to imply high melt/rock ratios during melt percolation (at least 17:1; Büchl et al., 2004b). The isotopic and geochemical compositions of SSZ dunites typically bear the characteristics of the melt and not the mantle residue (Büchl et al., 2002; Kelemen et al., 1992), in contrast to some dunites formed at mid-ocean ridge settings that instead preserve evidence for extreme melt depletion (e.g., Harvey et al., 2006). Büchl et al. (2002) reported generally higher Pt, Pd and Re in dunites than in spatially associated harzburgites for the Troodos ophiolite, Cyprus. The latter study invoked 'refertilisation' of the dunite layers to account for the compositions observed. By contrast, harzburgites are residues typically considered to form from more fertile peridotites by melt extraction and clinopyroxene dissolution at relatively low melt/rock ratios. The HSE abundances and Os isotope data of the Shetland dunites support the formation of dunite channels by melt percolation. Specifically, inter-element ratios (Fig. 5) and $\gamma_{Os492Ma}$ in many of the dunites span a considerably larger range of values than for associated harzburgites, consistent with imposition of a melt signature on the depleted dunite melt channels (Büchl et al., 2002, 2004a; Hanghøj et al., 2010).

Incongruent melting of sulphide-rich phases probably caused fractionation of the I-PGE from the P-PGE (Alard et al., 2000; Ballhaus et al., 2006; Bockrath et al., 2004; Luguet et al., 2003). The production of immiscible Cu–Ni-sulphide liquid, which concentrates Pt and Pd and is removed with the melt, leaves a monosulphide solution residue in which Os, Ir and Ru are preferentially retained (Liu et al., 2009). However, although useful to explain some of the Shetland HSE abundance patterns for dunites, this mechanism cannot solely account for the anomalous depletions in Ir and Pt observed in certain Shetland dunites (e.g., AV5, Fet 7). LA-ICP-MS in situ analysis of pentlandite in one sulphide-bearing dunite indicates that pentlandite (or Cr-spinel) does not have a primary control on Ir and Pt abundances in the Shetland peridotites. A possible alternative is that micro-grains of irarsite and Pt-alloys either formed early and were removed from the system, or concentrated into chromitite seams at the centres of dunite channels; these minerals have previously been reported from SOC chromitites (Prichard and Tarkian, 1988). In summary, the combined data suggest that the processes responsible for dunite formation were variably effective at mobilising the HSE, and that melting and associated sulphide mobilisation were complex in the Shetland peridotites.

*Melt-rock reaction and genesis of HSE-rich chromitite*

The numerous podiform chromitite seams and sulphide mineralisation zones present close to the petrological Moho in the SOC occur within dunite channels, suggesting that these features are related to melt-rock reaction during melt percolation (cf., Büchl et al., 2004b; Melcher et al., 1997; Uysal et al., 2009; Zhou et al., 1998). During mantle melting and the formation of olivine-rich residues, Cr behaves incompatibly, becoming sufficiently concentrated in the melt to crystallise only Cr-spinel and ultimately forms podiform chromitite through melt-rock reaction and/or magma mixing (Ballhaus, 1998; Matveev and Ballhaus, 2002; Melcher et al., 1997; O'Driscoll et al., 2010). The Cr contents of the SOC chromitites imply reaction with up to 400 times their mass in liquid, reflecting enhanced focused melt flow and excess melt/rock ratios (Kelemen et al., 1995; Leblanc and Ceuleneer, 1992). High degrees of fluid-assisted partial melting associated with SSZ ophiolites are understood to facilitate re-melting of already depleted mantle, allowing reprocessing of the oceanic upper mantle in SSZ settings (Brandon et al. 2000; Pearce et al., 1984). It is also interesting to note that the Shetland whole rock samples of dunites and harzburgites are not particularly deficient in $Cr_2O_3$ relative to peridotites from MORB-type ophiolites where chromitites are not developed, e.g., Taitao, Chile (Schulte et al., 2009). This suggests that the sourcing and fixing of Cr in chromitite seams in SSZ settings is not a localised effect, but involves large volumes of the surrounding upper mantle region.

Examination of three distinct chromitite zones close to the petrological Moho in the SOC reveals significant inter-seam compositional variability in terms of mineralogy, mineral compositions, HSE abundances and inter-element ratios, and Os isotope compositions. However, there is extremely limited intra-seam variability, as most compellingly observed in the restricted ranges of $\gamma_{Os492Ma}$ at Cliff, Harold's Grave, and Hagdale. These new observations enhance the argument of Büchl et al. (2004b) that ophiolite chromitites effectively homogenise the Os contribution of their different melt sources. Melt-rock reactions are considered to be important in the separation of immiscible base metal sulphides in dunites and chromitites (Büchl et al., 2002; Naldrett et al., 1990). The importance of sulphide distribution in upper mantle peridotites for the siting and mobilisation of the HSE is clear, due to the highly chalcophile nature of the HSE (e.g., Rudnick and Walker, 2009). In the Shetland rocks, sulphide (predominantly pentlandite) is present in both lithologies, but dominates in Cr-spinel-rich dunites, rather than chromitites. In each case however, the close textural association of Cr-spinel and sulphides suggests coeval formation, probably during the same melt percolation event.

Previous work has shown that I-PGE concentrations are dominant over the P-PGE in ophiolite chromitites, producing typical, negatively-sloping whole rock HSE patterns on chondrite-normalised diagrams that reflect melt extraction and incorporation of the moderately incompatible P-PGE into the melt phase (e.g., Melcher et al., 1997; Prichard and Lord, 1993; Uysal et al., 2009; Zhou et al.,1998). Harold's Grave and Hagdale chromitites are characterised by such patterns, but chromitite from the Cliff locality exhibits unusual HSE inter-element variations manifested by Pt and Pd enrichments (up to 253 $\mu g\, g^{-1}$), and a strongly positive trend on chondrite-normalised diagrams (Fig. 3). Enrichment in Pt and Pd in Cliff chromitites has been attributed previously to the effects of remobilisation and metasomatic scavenging of the HSE by sulphide, possibly related to the proximity of Cliff to the ophiolite sole thrust (Prichard and Lord, 1993), or another tectonic structure (Cutts et al., 2011). We suggest that the abundance of Ni-arsenide (over sulphide) at Cliff and the widespread alteration of Cr-spinel to 'ferritchromit' points to a post-serpentinisation oxidation event being responsible for mobilisation of the P-PGE from sulphide in the surrounding dunites at this locality.

The Shetland chromitites preserve a broad inventory of I-PGE- and P-PGE-bearing micron-scale mineral grains (Prichard and Tarkian, 1988; Prichard and Lord, 1993; Tarkian and Prichard, 1987). The I-PGE are hosted in minerals from the laurite-erlichmanite and irarsite-hollingworthite series, while the P-PGE are predominantly hosted in sperrylite and Pt–Pd–Cu $\pm$ Au alloys. These minerals are typically closely spatially associated with Ni-sulphides, such as pentlandite and Ni-arsenides. We find that chromium-spinel itself is a minor phase in controlling the HSE budget of the chromitites (and peridotites), in agreement with observations made on this and other ophiolites (Marchesi et al., 2010; Prichard and Tarkian, 1988; Prichard and Lord, 1993), though inclusions of laurite are observed in some Shetland chromitite Cr-spinels. In this context, it is notable that Ru concentrations are elevated in Cr-spinel crystals, in agreement with the conclusion of Tarkian and Prichard (1987) that laurite micro-inclusions commonly control Ru abundances.

Comparisons between plots of chondrite-normalised HSE abundances for whole rock peridotites and for in situ sulphide/arsenide analyses indicate that the chromitite HSE budget, including Re, can be satisfactorily accounted for by these phases in Cliff by ~60 mod% chromite and between 3 and 10 mod% Ni-arsenide (Fig. S4). The only HSE that does not reproduce well is Pt, which is about a factor of five too low in Ni-arsenide, implying possible retention within Pt-rich alloys or Pt-group mineral phases in the Cliff chromitites (e.g., sperrylite). Similar calculations for the Hagdale chromitites suggest that pentlandite hosts much of the HSE in this locality (Fig. S4). It is not possible to perform the same calculations for Harold's Grave as no sulphides or arsenides were identified in the chromitite sample analysed by LA-ICP-MS. However, laser-ablation traverses through the Cr-spinels and into the serpentinised matrix of the Harold's Grave chromitites show enhanced concentrations of some HSE. In particular, there is evidence for increased abundances of Os, Ru and Pd in the matrix (Fig. S4), presumably contained within HSE alloy grains, as these are favourably stabilised during serpentinisation.

*Mantle Os isotope evolution: chromitites or peridotites?*

The combination of chromitites and peridotites analysed from the SOC records significant isotopic heterogeneity at 492 Ma (Fig. 4), as also revealed by $T_{RD}$ model ages of up to 1.4 Ga (Table 1). Rhenium–Os isotope studies of ophiolites from 1.95 Ga to present-day (e.g., Büchl et al., 2004a; Schulte et al., 2009; Tsuru et al., 2000; Walker et al., 1996), together with Os isotopic data from modern abyssal and fore-arc peridotites (e.g., Harvey et al., 2006; Liu et al., 2009; Meibom and Frei, 2002; Parkinson et al., 1998; Walker et al., 2005), suggest a limited, yet significant, percentage of rocks with Proterozoic to Archaean model melt depletion ages, indicating that small (sub-m-scale) rhenium–depleted domains can survive in the DMM for geologically significant timescales (Harvey et al., 2006; Liu et al., 2009; Parkinson et al., 1998; Schulte et al., 2009). Thus, the sub-chondritic Os isotope ratios preserved in some SOC harzburgites attest to mantle processing prior to the 492 Ma formation age, supporting previous suggestions of ancient melt depletion, possibly related to episodic major melting events. This depletion is a common feature of the oceanic upper lithosphere (Alard et al., 2005; Harvey et al., 2006; Marchesi et al., 2010; Murphy et al., 2011; Pearson et al., 2007).

In the case of the Shetland peridotites, Iapetus Ocean formation is believed to have been initiated at ~620 Ma (Woodcock and Strachan, 2000), implying that melt depleted domains can survive complete ocean basin cycles. To highlight the sub-m scale at which these domains occur, it is useful to consider that the Shetland harzburgite with the $T_{RD}$ age of 1.4 Ga (*V6*) ($\gamma_{Os492Ma} = -5.3$) comes from a sequence of layered rocks in which a dunite (*V1*) with $\gamma_{Os492Ma} = +1.3$, was sampled less than one metre away. Similar m-to-sub-cm scales of mantle compositional heterogeneity have been illustrated by Marchesi et al. (2010), who documented the control that sub-mm chromitite-hosted platinum-group alloy grains have on the Os isotopic heterogeneity preserved in the Mayarí-Cristal ophiolite (Cuba). They argued that the presence of such heterogeneities reflects the original Os isotopic heterogeneity of the mantle source and that chromitite formation had not, in this instance, completely homogenised the Os contributions of the different source melts.

Walker et al. (2002) analysed chromitites from ophiolites of different ages from diverse tectonic settings worldwide, with the goal of deducing the average $^{187}Os/^{188}Os$ composition of the convecting upper mantle. Chromitites were chosen for this task based on their typically excellent states of preservation in ophiolites, as well as their characteristically very low Re/Os, resulting in minimal age corrections to time of formation. They reported a well-defined average $^{187}Os/^{188}Os$ value of $0.12809 \pm 0.00085$ ($2\sigma$), when data for Phanerozoic ophiolite chromitites are projected to the present. These authors suggested that this value is representative of the DMM and argued that the addition of radiogenic Os from the dehydrating oceanic crust has had little effect on the Os isotopic composition of the chromitites. Büchl et al. (2004b) reported a similar average chromitite Os isotopic composition of $0.1284 \pm 0.0021$ ($2\sigma$) from the Troodos ophiolite and calculated that melt-rock ratios of approximately 17:1 would be required to raise the average Troodos ophiolite peridotite $^{187}Os/^{188}Os$ ratio (0.127, Os 4.2 ng $g^{-1}$) to this value. The latter authors argued that melt percolation models for the formation of podiform chromitites do not permit their Os isotopic composition being used as a good average for the DMM; rather they probably reflect its upper limit. Although the number of data available for SOC peridotites is still limited, it is useful to make some comparisons of average $\gamma_{Os492Ma}$ among the broad classes of rocks analysed. The average $\gamma_{Os492Ma}$ value for the dunites and the harzburgites combined (*sans* Fet 3 and 4) is $+1.1 \pm 8.2$. The harzburgites alone average $-0.5 \pm 4.4$ ($n=15$) while the dunites average $+3.9 \pm 9.9$ ($n=9$). Although the two sigma standard deviations quoted above highlight the large total range of $\gamma_{Os492Ma}$ for the Shetland peridotites (Table 1), the dunites are more radiogenic compared to the harzburgites, as observed for other ophiolites (e.g., Büchl et al., 2004b).

The three Shetland chromitites preserve significant Os isotopic variability at 492 Ma, ranging from sub-chondritic to supra-chondritic compositions, though within individual localities the Os isotope compositions are quite restricted. It is also worth noting that for a given chromitite locality, chromitite $\gamma_{Os492Ma}$ values may be significantly more radiogenic than the spatially associated dunite (e.g., Hagdale; Table 1). The average $\gamma_{Os492Ma}$ value for the chromitites is $+2.4 \pm 3.0$ ($n=12$), which is notably higher than the harzburgites, but lower than the dunite average. Given these observations and the complementary variations observed in the HSE chondrite-normalised patterns described above, it seems that the compositions of ophiolite chromitites are strongly influenced by the degree to which the melt extracted from the surrounding peridotites interacts with slab-derived Si- and/or $H_2O$-rich magmas (Ballhaus, 1998; Melcher et al., 1997). Thus, the Os isotopic composition of ophiolite chromitites probably represents only upper constraints on the composition of convecting upper mantle (Walker et al., 2002).

Overall, the Os isotopic composition of the SOC, assuming that this value is represented by the average $\gamma_{Os492Ma}$ for the harzburgites of $-0.5$, falls between estimates for DMM evolution based on abyssal peridotites ($\gamma_{Os492Ma} \sim -2$ when projected back in time to 492 Ma; Snow and Reisberg, 1995) and ophiolite chromitites ($\sim +1$). Thus, the data for the SOC suggest an Os isotopic composition representative of this mantle section that is between the estimates based on abyssal peridotites (e.g., Snow and Reisberg, 1995) and ophiolite chromitites (e.g. Walker et al., 2002). Using the assumptions applied by Walker et al. (2002), that the convecting upper mantle comprises 50% of the total mass of the mantle, and that the average isolation period for subducted oceanic crust is 1.5 to 2.0 Ga, the lower estimated $^{187}Os/^{188}Os$ for the convecting mantle would mean that the bulk mantle harbours subducted mafic oceanic crust that comprises 3–4% of the total mass of the mantle, and that this recycled crust remains isolated from the convecting upper mantle.

*Enigmas of mantle melt depletion and (auto?)-refertilisation*

The relationship between major element components such as $Al_2O_3$ and $^{187}Os/^{188}Os$ is useful for tracking melt extraction and

refertilisation, given the incompatible nature of $Al_2O_3$ and Re, and the high compatibility of Os in peridotite residues. Schulte et al. (2009) proposed a two stage melting model for the mantle rocks preserved in the ~6 Ma Taitao ophiolite to explain the $^{187}Os/^{188}Os$ versus $Al_2O_3$ relationship that they observed. The first, ancient (Proterozoic) melt depletion event removed Re proportional to the amount of melt extraction and was responsible for the observed range in $^{187}Os/^{188}Os$. The second, recent melting event further depleted the peridotites in $Al_2O_3$ (and Re) without significantly disturbing the Os isotopes, or perplexingly, Re/Os. An important implication drawn from Schulte et al. (2009) was that convection in the DMM was not particularly effective at homogenising Os isotopes over >1000 Ma.

In contrast to the Taitao ophiolite (Schulte et al., 2009), and abyssal peridotites for which Os isotopic and bulk composition data are available (e.g., Liu et al. 2009), there is no apparent relation between $^{187}Os/^{188}Os$ and indicators of melt depletion, such as bulk rock $Al_2O_3$, for the SOC peridotites (Fig. 6). Further, although not as depleted in $Al_2O_3$, peridotites from the Troodos and Oman ophiolites have similar ranges in initial $\gamma_{Os}$ (Büchl et al., 2004b; Hanghøj et al., 2010) without obvious correlations with $Al_2O_3$ (Fig. 6). In the SOC suite, some of the harzburgites have PM-like HSE abundances, yet are characterised by having low $Al_2O_3$ contents. A key question is, assuming derivation from an original protolith with a primitive mantle composition, how $Al_2O_3$ was lost without strongly modifying the relative and absolute abundances of the HSE? Consideration of the tectonic setting within which these ophiolites have been emplaced might be the first step in unravelling this complexity. A recent comprehensive overview of global ophiolite occurrences classified Taitao as a mid-ocean ridge ophiolite, in contrast to the Troodos and Oman ophiolites, which were classified as SSZ type (Dilek and Furnes, 2011). Although not included in that study, there is little doubt that the SOC would also fall into the SSZ category, given the geochemical and field-based evidence presented above. The implications of this are that SSZ ophiolites develop significantly greater chemical and isotopic heterogeneities during melting as recorded in $^{187}Os/^{188}Os$ versus $Al_2O_3$, possibly as a consequence of enhanced fluid fluxing, than are recorded in ophiolites from other tectonic settings. This comparison offers insight into the way in which tectonic setting controls the style of mantle melting and evolution

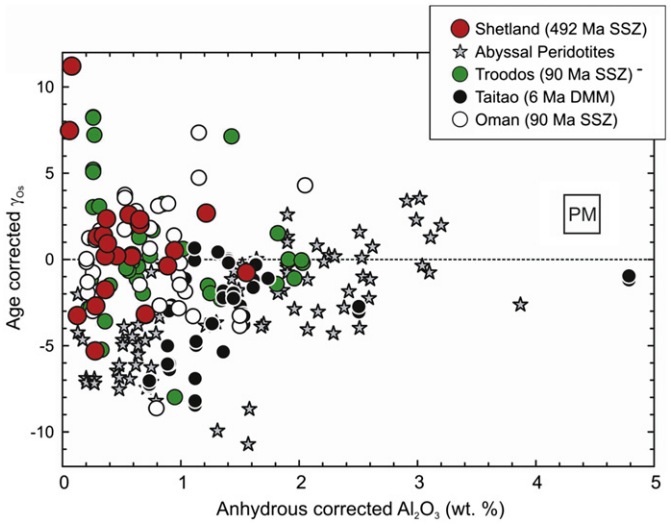


**Fig. 6.** Plot of $\gamma_{Os492Ma}$ vs. $Al_2O_3$ (wt% anhydrous corrected) for Shetland Ophiolite Complex peridotites. Also plotted are data from the Taitao (Chile; Schulte et al., 2009), Troodos (Cyprus; Büchl et al., 2004a) and Oman (Hanghøj et al., 2010) Ophiolites as well as abyssal peridotite data from Liu et al. (2009) and references therein. See Section 5.5 for further discussion.

of the Os isotope and HSE composition of the associated mantle. Fig. 6 shows that the Taitao data of Schulte et al. (2009) are contained within the $\gamma_{Os492Ma}$ versus $Al_2O_3$ space occupied by abyssal peridotites, suggesting that long term melt extraction from the DMM may account for the compositions of both. However, Troodos, Oman and particularly the Shetland peridotite compositions extend to much more radiogenic Os isotope compositions at low $Al_2O_3$ (Fig. 6). This is not a refertilisation effect, which might be expected to also reintroduce $Al_2O_3$ into already depleted peridotites, but may instead be a function of melt percolation and melt-rock reaction during fluid-assisted mantle melting, where the dunite channels have accommodated radiogenic mantle melts that have in turn imparted relatively high $^{187}Os/^{188}Os$ to the rocks.

Whattam and Stern (2011) have suggested that ophiolites may preserve evidence for multiple styles (degrees) of partial melting, as a subduction zone evolves from initiation to maturity and ultimately undergoes enhanced melting as a result of interaction with fluids derived from the down-going dehydrating oceanic crust and sediments. Such models might explain why some ophiolites (e.g., Troodos, Oman and Shetland) contain evidence of multiple stages of melting (Dilek and Furnes, 2011). In addition to preserving cm-scale domains that record a Mesoproterozoic melting event, the Shetland peridotites also preserve cm-to-m scale heterogeneities in their Os isotopes and HSE abundances developed during Iapetan Ocean upper mantle SSZ melt extraction. It is clear, therefore, that in some instances common single-stage melt extraction models for ophiolite peridotites may vastly underestimate the complexity of the processes involved in such settings.

## Conclusions

Despite pervasive serpentinisation, SOC peridotites and chromitites generally retain their primary magmatic Re–Os isotope signatures and HSE abundances. Dunites reveal more radiogenic Os isotope compositions than associated interlayered harzburgites, a characteristic inherited as a consequence of greater interaction with percolating melts during SSZ-type melt extraction. The presence of podiform chromitite seams within many dunite lenses and layers, together with evidence that individual chromitites preserve initial (~492 Ma) Os isotopic heterogeneity and HSE abundance variations, further highlights the importance of melt-rock reaction and percolation in SSZ mantle settings. The dichotomy present in the Os isotopic compositions of SOC chromitites versus harzburgites indicates that the latter lithology may not be a suitable proxy for the average $^{187}Os/^{188}Os$ composition of the bulk convecting upper mantle. Comparisons drawn in this study between the Os isotopic compositions of SOC peridotites and those of other well known ophiolite peridotites underline the importance of fluid-assisted mantle melting in the development of the cm-to-m scale Os isotope heterogeneities often found in the oceanic mantle.

## Acknowledgements

Grants to B.O'D from the Mineralogical Society of Great Britain and Ireland, the Geological Society of London, the Geological Society of Edinburgh, and the Royal Society supported this work. Support from the Maryland Nanocenter and NISP laboratory for maintaining the electron microprobe analyser is acknowledged. We thank Jude Coggon, an anonymous reviewer and the editor, Bernard Marty, for constructive review comments. We also acknowledge Nigel for stimulating tales of sheep-shearing, bar-

tending and lighthouse-mending, and making our stay on Unst a memorable one.

## Appendix A. Supplementary material

Supplementary data associated with this article can be found in the online version at http://dx.doi.org/10.1016/j.epsl.2012.03.035.

## References


Alard, O., Griffin, W.L., Lorand, J.P., Jackson, S.E., O'Reilly, S.Y., 2000. Non-chondritic distribution of the highly siderophile elements in mantle sulphides. Nature 407, 891–894.

Alard, O., Luguet, A., Pearson, N.J., Griffin, W.L., Lorand, J.-P., Gannoun, A., Burton, K.W., O'Reilly, S.Y., 2005. In situ Os isotopes in abyssal peridotites bridge the isotopic gap between MORBs and their source mantle. Nature 436, 1005–1008.

Allègre, C.J., Luck, J.M., 1980. Osmium isotopes as petrogenetic and geological tracers. Earth Planet. Sci. Lett. 48, 148–154.

Ballhaus, C., 1998. Origin of podiform chromite deposits by magma mingling. Earth. Planet. Sci. Lett. 156, 185–193.

Ballhaus, C., Bockrath, C., Wohlgemuth-Ueberwasser, C., Vera Laurenz, V., Berndt, J., 2006. Fractionation of the noble metals by physical processes. Contrib. Mineral. Petrol. 152, 667–684.

Becker, H., Horan, M.F., Walker, R.J., Gao, S., Lorand, J.-P., Rudnick, R.L., 2006. Highly siderophile element composition of the Earth's primitive upper mantle: Constraints from new data on peridotite massifs and xenoliths. Geochim. Cosmochim. Acta 70, 4528–4550.

Bockrath, C., Ballhaus, C., Holzheid, A., 2004. Fractionation of the platinum-group elements during mantle melting. Science 305, 1951–1953.

Brandon, A.D., Snow, J.E., Morgan, J.W., Mock, T.D., 2000. $^{190}Pt$–$^{186}Os$ and $^{187}Re$–$^{187}Os$ systematics of abyssal peridotites. Earth. Planet. Sci. Lett. 177, 319–335.

Büchl., A., Brügmann, G., Batanova, V.G., Münker, C., Hofmann, A.W., 2002. Melt percolation monitored by Os isotopes and HSE abundances: a case study from the mantle section of the Troodos Ophiolite. Earth. Planet. Sci. Lett. 204, 385–402.

Büchl, A., Brügmann, G., Batanova, V.G., Hofmann, A.W., 2004a. Os mobilization during melt percolation: the evolution of Os isotope heterogeneities in the mantle sequence of the Troodos ophiolite, Cyprus. Geochim. Cosmochim. Acta 68, 3397–3408.

Büchl, A., Brügmann, G., Batanova, V.G., 2004b. Formation of podiform chromitite deposits: implications from PGE abundances and Os isotopic compositions of chromites from the Troodos complex. Cyprus. Chem. Geol 208, 217–232.

Chew, D.M., Daly, J.S., Magna, T., Page, L.M., Kirkland, C.L., Whitehouse, M.J., Lam, R., 2010. Timing of ophiolite obduction in the Grampian orogen. Geol. Soc. Amer. Bull. 122, 1787–1799.

Cutts, K.A., Hand, M., Kelsey, D.E., Strachan, R.A., 2011. P–T constraints and timing of Barrovian metamorphism in the Shetland Islands, Scottish Caledonides: implications for the structural setting of the Unst ophiolite. J. Geol. Soc. Lond. 168, 1265–1284.

Day, J.M.D., Pearson, D.G., Hulbert, L.J., 2008. Rhenium-osmium isotope and platinum-group element constraints on the origin and evolution of the 1.27 Ga Muskox layered intrusion. J. Petrol. 49, 1255–1295.

Day, J.M.D., Walker, R.J., James, O.B., Puchtel, I.S., 2010. Osmium isotope and highly siderophile element systematics of the lunar crust. Earth Planet. Sci. Lett. 289, 595–605.

Dick, H.J.B., Fisher, R.L., Bryan, W.B., 1984. Mineralogic variability of the uppermost mantle along mid-ocean ridges. Earth Planet. Sci. Lett. 69, 88–106.

Dilek, Y., Furnes, H., 2011. Ophiolite genesis and global tectonics: Geochemical and tectonic fingerprinting of ancient oceanic lithosphere. Geol. Soc. Am. Bull. 123, 387–411.

Droop, G.T.R., 1987. A general equation for estimating $Fe^{3+}$ concentrations in ferromagnesian silicates and oxides from microprobe analyses, using stoichiometric criteria. Mineral. Mag. 51, 431–435.

Dupré, B., Allègre, C.J., 1983. Lead-strontium isotope variation in Indian Ocean basalts and mixing phenomena. Nature 303, 142–146.

Elthon, D., 1991. Geochemical evidence for formation of the Bay of Islands Ophiolite above a subduction zone. Nature 354, 140–143.

Flinn, D., 2001. The basic rocks of the Shetland Ophiolite Complex and their bearing on its genesis. Scotl. J. Geol 37 (2), 79–96.

Flinn, D., Oglethorpe, R.J.D., 2005. A history of the Shetland Ophiolite Complex. Scotl. J. Geol. 41 (2), 141–148.

Flinn, D., Miller, J.A., Roddam, D., 1991. The age of the Norwick hornblendic schists of Unst and Fetlar and the obduction of the Shetland ophiolite. Scotl. J. Geol 27, 11–19.

Gannoun, A., Burton, K.W., Parkinson, I.J., Alard, O., Schiano, P., Thomas, L.E., 2007. The scale and origin of the osmium isotope variation in mid-ocean ridge basalts. Earth Planet. Sci. Lett. 259, 541–556.

Hanghøj, K., Kelemen, P.B., Hassler, D., Godard, M., 2010. Composition and genesis of depleted mantle peridotites form the Wadi Tayin Massif, Oman ophiolite; major and trace element geochemistry, and Os isotope and PGE systematics. J. Petrol. 51, 201–227.

Harvey, J., Gannoun, A., Burton, K.W., Rogers, N.W., Alard, O., Parkinson, I.J., 2006. Ancient melt extraction from the oceanic upper mantle revealed by Re–Os isotopes in abyssal peridotites from the Mid-Atlantic ridge. Earth Planet. Sci. Lett. 244, 606–621.

Horan, M.F., Walker, R.J., Morgan, J.W., Grossman, J.N., Rubin, A.E., 2003. Highly siderophile elements in chondrites. Chem. Geol. 196, 27–42.

Kelemen, P.B., Dick, H.J.B., Quick, J.E., 1992. Formation of harzburgite by pervasive melt/rock reaction in the upper mantle. Nature 358, 635–641.

Kelemen, P.B., Shimizu, N., Salters, V.J.M., 1995. Extraction of mid-ocean-ridge basalt from upwelling mantle by focused flow of melt in dunite channels. Nature (375), 747–753.

Lago, B.L., Rabinowicz, M., Nicolas, A., 1982. Podiform chromitite ore bodies: a genetic model. J. Petrol. 23, 103–125.

Leblanc, M., Ceuleneer, G., 1992. Chromite crystallization in a multicellular magma flow: evidence from a chromitite dike in the Oman ophiolite. Lithos 27, 231–257.

Liu, C.-Z., Snow, J.E., Brügmann, G., Hellebrand, E., Hofmann, A.W., 2009. Non-chondritic HSE budget on Earth's upper mantle evidenced by abyssal peridotites from Gakkel ridge (Arctic Ocean). Earth Planet. Sci. Lett. 283, 122–132.

Lorand, J.P., Keays, R.R., Bodinier, J.L., 1993. Copper and noble-metal enrichments across the lithosphere asthenosphere boundary of mantle diapirs—evidence from the Lanzo Lherzolite Massif. J. Petrol. 34, 1111–1140.

Luck, J.M., Allègre, C.J., 1991. Osmium isotopes in ophiolites. Earth Planet. Sci. Lett. 107, 406–415.

Luguet, A., Lorand, J.P., Seyler, M., 2003. Sulfide petrology and highly siderophile element geochemistry of abyssal peridotites: a coupled study of samples from the Kane Fracture Zone (45° W 23°20 N, MARK Area, Atlantic Ocean). Geochim. Cosmochim. Acta 67, 1553–1570.

Luguet, A., Shirey, S.B., Lorand, J.-P., Horan, M.F., Carlson, R.W., 2007. Residual platinum group minerals from highly depleted harzburgites of the Lherz massif (France) and their role in HSE fractionation of the mantle. Geochim. Cosmochim. Acta 71, 3082–3097.

Marchesi, C., Gonzalez-Jimenez, J.M., Gervilla, F., Garrido, C.J., Griffin, W.L., O'Reilly, S.Y., Proenza, J.A., Pearson, N.J., 2010. In situ Re–Os isotopic analysis of platinum-group minerals from the Mayari-Cristal ophiolitic massif (Mayari-Baracoa ophiolitic belt, eastern Cuba): implications for the origin of Os-isotope heterogeneities in podiform chromitites. Contrib. Mineral. Petrol. 161 (6), 977–990.

Matveev, S., Ballhaus, C., 2002. Role of water in the origin of podiform chromitite deposits. Earth Planet. Sci. Lett. 203, 235–243.

Meibom, A., Frei, R., 2002. Evidence for an ancient osmium isotopic reservoir in Earth. Science 296, 516–518.

Melcher, F., Grum, W., Simon, G., Thalhammer, T.V., Stumpel, E.F., 1997. Petrogenesis of the ophiolitic giant chromite deposits of Kempirsai, Kazakhstan: a study of solid and fluid inclusions in chromite. J. Petrol. 38 (10), 1419–1458.

Murphy, J.B., Cousens, B.L., Braid, J.A., Strachan, R.A., Dostal, J., Keppie, J.D., Nance, R.D., 2011. Highly depleted oceanic lithosphere in the Rheic Ocean; Implications for Paleozoic plate reconstructions. Lithos 123, 165–175.

Naldrett, A.J., Brugmann, G.E., Wilson, A.H., 1990. Models for the concentration of PGE in layered intrusions. Can. Mineral 28, 389–408.

O'Driscoll, B., Day, J.M.D., Daly, J.S., Walker, R.J., McDonough, W.F., 2009. Rhenium-osmium isotope and platinum-group elements in the Rum Layered Suite, Scotland: Implications for Cr-spinel seam formation and the composition of the Iceland mantle anomaly. Earth Planet. Sci. Lett 286, 41–51.

O'Driscoll, B., Emeleus, C.H., Donaldson, C.H., Daly, J.S., 2010. Cr-spinel seam petrogenesis in the Rum Layered Suite, NW Scotland: cumulate assimilation and in situ crystallisation in a deforming crystal mush. J. Petrol. 51, 1171–1201.

Parkinson, I.J., Hawkesworth, C.J., Cohen, A.J., 1998. Ancient mantle in a modern arc: osmium isotopes in Izu-Bonin-Mariana forearc peridotites. Science 281, 2011–2013.

Pearce, J.A., Lippard, S.J., Roberts, S., 1984. Characteristics and tectonic significance of supra-subduction zone ophiolites. In: Kokelaar, B.P., Howells, M.F. (Eds.), Marginal Basin Geology. Geological Society Special Publication, pp. 16, 77–94.

Pearce, J.A., 2003. Supra-subduction zone ophiolites: the search for modern analogues. In: Dilek, Y., Newcomb, S (Eds.), Ophiolite Concept and the Evolution of Geological Thought. Geological Society of America Special Paper 373, pp. 269–293.

Pearson, D.G., Parman, S.W., Nowell, G.M., 2007. A link between large mantle melting events and continent growth seen in Osmium isotopes. Nature 449, 202–205.

Prichard, H.M., Lord, R.A., 1993. An overview of the PGE concentrations in the Shetland ophiolite complex. In: Prichard, H.M., Alabaster, T., Harris, N.B.W., Neary, C.R. (Eds.), Magmatic Processes and Plate Tectonics. Geol. Soc. Spec. Pub., pp. 273–294. No. 76.

Prichard, H.M., Lord, R.A., Neary, C.R., 1996. A model to explain the occurrence of platinum- and palladium-rich ophiolite complexes. J. Geol. Soc. Lond. 153, 323–328.

Prichard, H.M., Tarkian, M., 1988. Platinum and palladium minerals from two PGE-rich localities in the Shetland Ophiolite Complex. Can. Mineral 26, 979–990.

Puchtel, I.S., Walker, R.J., James, O.B., Kring, D.A., 2008. Osmium isotope and highly siderophile element systematics of lunar impact melt breccias: implications

for the late accretion history of the Moon and Earth. Geochim. Cosmochim. Acta 72, 3022–3042.
Quick, J.E., 1981. Petrology and petrogenesis of the Trinity peridotite, an upper mantle diapir in the eastern Klamath mountains, northern California. J. Geophys. Res 86, 1837–1863.
Reisberg, L., Zindler, A., 1986. Extreme isotopic variations in the upper mantle: evidence from Rhonda. Earth. Planet. Sci. Lett. 81, 29–45.
Roy-Barman, M., Allègre, C.J., 1994. $^{187}Os/^{186}Os$ ratios of mid ocean ridge basalts and abyssal peridotites. Geochim. Cosmochim. Acta 58, 5043–5054.
Rudnick, R.L., Walker, R.J., 2009. Interpreting ages from Re–Os isotopes in peridotites. Lithos 1125, 1083–1095.
Sato, H., Ogawa, Y., 2000. Sulfide minerals as an indicator for petrogenesis and serpentinization of peridotites: an example from the Hayama–Mineoka belt, central Japan. In: Dilek, Y., Moores, E.M., Elthon, D., Nicolas, A. (Eds.), Ophiolites and Oceanic Crust; New insights from field studies and the Ocean Drilling Program: Boulder, Colarado, Geological Society of America Special Paper 349, pp. 419–429.
Schiano, P., Birck, J.-L., Allègre, C.J., 1997. Osmium–strontium–neodymium–lead isotopic covariations in mid-ocean ridge basalt glasses and the heterogeneity of the upper mantle. Earth Planet. Sci. Lett. 150, 363–379.
Schulte, R.F., Schilling, M., Anma, R., Farquhar, J., Horan, M.F., Komiya, T., Piccoli, P.M., Pitcher, L., Walker, R.J., 2009. Chemical and chronologic complexity in the convecting upper mantle: Evidence from the Taitao ophiolite, southern Chile. Geochim. Cosmochim. Acta 73, 5793–5819.
Sharma, M., Wasserburg, G.J., 1996. The neodymium isotopic compositions and rare earth patterns in highly depleted ultramafic rocks. Geochim. Cosmochim. Acta 60, 4537–4550.
Shi, R., Alard, O., Zhi, X., O'Reilly, S.Y., Pearson, N.J., Griffin, W.L., Zhang, M., Chen, X., 2007. Multiple events in the Neo-Tethyan oceanic upper mantle: Evidence from Ru–Os–Ir alloys in the Luobusa and Dongqiao ophiolitic podiform chromitites, Tibet. Earth. Planet. Sci. Lett. 261 (1–2), 33–48.
Snow, J.E., Hart, S.R., Dick, H.J.B., 1994. Nd and Sr isotopic evidence for a link between mid-ocean ridge basalts and abyssal peridotites. Nature 371, 57–60.
Snow, J.E., Reisberg, L., 1995. Os isotopic systematics of the MORB mantle: results from altered abyssal peridotites. Earth Planet. Sci. Lett. 133, 411–421.
Snow, J.E., Schmidt, G., 1998. Constraints on Earth accretion deduced from noble metalsin the oceanic mantle. Nature 391, 166–169.
Spray, J.G., 1988. Thrust-related metamorphism beneath the Shetland Islands oceanic fragment, northeast Scotland. Can. J. Earth Sci. 25, 1760–1776.
Spray, J.G., Dunning, G.R., 1991. A U/Pb age for the Shetland Islands oceanic fragment, Scottish Caledonides: evidence from anatectic plagiogranites in 'layer 3' shear zones. Geol. Mag. 128 (6), 667–671.
Standish, J.J., Hart, S.R., Blusztain, J., Dick, H.J.B., 2002. Abyssal peridotite osmium isotopic compositions from Cr-spinel. G-cubed 3, 1004, http://dx.doi.org/10.1029/2001GC000161.
Tarkian, M., Prichard, H.M., 1987. Irarsite-hollingworthite solid-solution series and other associated Ru-, Os-, Ir-, and Rh-bearing PGM's from the Shetland ophiolite complex. Miner. Dep. 22, 178–184.
Tsuru, A., Walker, R.J., Kontinen, A., Peltonen, P., Hanski, E., 2000. Re–Os isotopic systematics of the 1.95 Ga Jormua Ophiolite Complex, northeastern Finland. Chem. Geol. 164, 123–141.
Uysal, I., Tarkian, M., Sadiklar, M.B., Zaccarini, F., Meisel, T., Garuti, G., Heidrich, S., 2009. Petrology of Al- and Cr-rich ophiolitic chromitites from the Muğla, SW Turkey: implications from composition of chromite, solid inclusions of platinum-group mineral, silicate, and base-metal mineral, and Os-isotope geochemistry. Contrib. Mineral. Petrol. 158 (5), 659–674.
Walker, R.J., Shirey, S.B., Boyd, F.R., 1989. Os, Sr, Nd, and Pb isotope systematics of Southern African peridotite xenoliths; implications for the chemical evolution of subcontinental mantle. Geochim. Cosmochim. Acta 53, 1583–1595.
Walker, R.J., Hanski, E.J., Vuollo, J., Liipo, J., 1996. The Os isotopic composition of Proterozoic upper mantle: evidence for chondritic upper mantle from the Outokumpu ophiolite, Finland. Earth. Planet. Sci. Lett. 141, 161–173.
Walker, R.J., Prichard, H.M., Ishiwatari, A., Pimentel, M., 2002. The osmium isotopic composition of convecting upper mantle deduced from ophiolite chromites. Geochim. Cosmochim. Acta 66, 329–345.
Walker, R.J., Brandon, A.D., Bird, J.M., Piccoli, P.M., McDonough, W.F., Ash, R.D., 2005. $^{186}Os$-$^{187}Os$ systematics of Os–Ir–Ru alloy grains, southwestern Oregon. Earth. Planet. Sci. Lett. 230, 211–226.
Walker, R.J., 2009. Highly siderophile elements in the Earth, Moon and Mars: Update and implications for planetary accretion and differentiation. Chem. Erde 69, 101–125.
Whattam, S.A., Stern, R.J., 2011. The 'subduction initiation rule': a key for linking ophiolites, intra-oceanic forearcs, and subduction initiation. Contrib. Mineral. Petrol. 162 (5), 1031–1045.
Woodcock, N.H., Strachan, R., 2000. Geological History of Britain and Ireland. Blackwell Science, Oxford.
Workman, R.K., Hart, S.R., 2005. Major and trace element composition of the depleted MORB mantle (DMM). Earth Planet. Sci. Lett. 231, 53–72.
Zhou, M.-F., Sun, M., Keays, R.R., Kerrich, R.W., 1998. Controls of platinum-group elemental distributions of podiform chromitites: a case study of high-Cr and high-Al chromitites from Chinese orogenic belts. Geochim. Cosmochim. Acta 62, 677–688.